Manuscript prepared for Atmos. Chem. Phys. Discuss.
with version 4.1 of the LaTeX class copernicus_discussions.cls.
Date: 18 September 2014

Lidar observation of the 2011 Puyehue-Cordón Caulle volcanic aerosols at Lauder, New Zealand

K. Nakamae[1], **O. Uchino**[1], **I. Morino**[1], **B. Liley**[2], **T. Sakai**[3], **T. Nagai**[3], **and T. Yokota**[1]

[1]National Institute for Environmental Studies, Tsukuba, Ibaraki, Japan
[2]National Institute of Water and Atmospheric Research, Lauder, New Zeal and
[3]Meteorological Research Institute, Tsukuba, Ibaraki, Japan

Correspondence to: K. Nakamae (nakamae.kumi@nies.go.jp)

Abstract

On 4 June 2011, the Puyehue-Cordón Caulle volcanic complex (40.6° S, 72.1° W) in Chile erupted violently and injected volcanic aerosols into the atmosphere. For the safety of civil aviation, continuous lidar observations were made at Lauder, New Zealand (45.0° S, 169.7° E), from 11 June through 6 July 2011. The purpose of our study is to quantify the influence of the volcanic ejections from large eruption, and we use the data from the ground-based lidar observation. We analyzed lidar data at a wavelength of 532 nm and derived the backscattering ratio and depolarization ratio profiles. During June and July, within the altitude range of 10–15 km, the volcanic aerosols had high depolarization ratios (20–35 %), an indication of non-spherical volcanic ash particles. The time series of the backscattering ratio during continuous observations had three peaks occurring at about 12 day intervals: 26.7 at 11.2 km on 11 June, 18.1 at 12.0 km on 23 June, and 5.3 at 11.1 km on 6 July. The optical depth of the volcanic aerosols was 0.45 on 11 June, when the continuous lidar observation started, 0.31 on 23 June, and 0.12 on 6 July. The depolarization ratio values remained high up to a month after the eruption and the small wavelength exponent calculated from the backscattering coefficients at 532 nm and 1064 nm suggest that a major constituent of the volcanic aerosols was large, non-spherical particles. The presence of volcanic ash in the stratosphere might affect the error in Greenhouse gases Observing SATellite (GOSAT) XCO_2 retrieval using the 1.6 μm band. We briefly discuss the influence of the increased aerosols on GOSAT products.

1 Introduction

Eruptions with a volcanic explosivity index (VEI) larger than 4 to 5 are generally expected to inject volcanic aerosols into the stratosphere (Newhall and Self, 1982; Deshler, 2008; Vernier et al., 2011; Trickl et al., 2013). The VEI was developed as a simple and semi-quantitative scheme for estimating the magnitude of historic eruptions by Newhall and Self (1982). Eruptions are assigned to a VEI on a scale of 0 to 8, using the criteria such as the volume of ejecta, column height and qualitative of the eruption. Especially, the volume of ejecta and the column

height are important. Volcanic aerosol particles larger than 10 μm injected into the stratosphere settle rapidly, so their climatic effects can generally be neglected (Robock, 2000). Volcanic ash is known to affect tropospheric cloud phases by acting as ice nuclei (Durant et al., 2008; Lathem et al., 2011). In contrast, when a large amount of sulfur dioxide is injected into the stratosphere, it is converted to sulfuric acid particles within several weeks (Zhao et al., 1995). The Mt. Pinatubo volcano (Philippines, 15.1° N; 120.4° E) erupted on 15 June 1991 and stratospheric injection of about 20 Mt of SO_2 was detected by the Total Ozone Mapping Spectrometer (Bluth et al., 1992). The SO_2 is oxidized to sulfuric acid vapor from which sulfuric acid particles are produced by homogeneous nucleation (Wu et al., 1994). These particles are long-lived in the stratosphere (Uchino et al., 1995; Nagai et al., 2010), depending on the latitude and altitude of injection, and significantly affect the global climate and radiation budget and the ozone layer (Minnis et al., 1993; McCormick et al., 1995; Alados-Arboledas et al., 1997; Robock, 2000; Solomon et al., 2011).

Large amounts of volcanic ash in the atmosphere can damage aircraft engines and raise flight safety concerns; as a result they can have significant consequences for air traffic. The volcanic hazards for aircraft have been recognized that are the stop of aviation engines, reduction of visibility and the damage to windshield due to volcanic ash (Bernard and Rose, 1990). For example, the ash plume from the eruption of the Eyjafjallajökull volcano (63.63° N, 19.62° W, Iceland) on 14 April 2010 disrupted air traffic over Europe. The small particles and trace gases such as SO_2 from this eruption were transported over long distances (Tesche et al., 2010; Ansmann et al., 2010; Wiegner et al., 2012).

On 4 June 2011, the Puyehue-Cordón Caulle Volcanic Complex (hereafter PCCVC; 40.59° S, 72.11° W) in Chile erupted and injected large amounts of volcanic ash particles into the atmosphere (VEI=3) (Dzierma and Wehrmann, 2012). This volcanic complex had previously erupted in May 1960 (Lara et al., 2004; Raga et al., 2013). The volcanic aerosol plumes travelled eastward from Chile via the prevailing westerlies and passed over New Zealand (Klüser et al., 2013). Because the Volcanic Ash Advisory Center (VAAC) in Wellington had forecast that a large volcanic aerosol plume would reach New Zealand, we performed continuous observations of volcanic aerosols with lidar at Lauder (45.04° S, 169.68° E), New Zealand, and provided

the observational data to the VAAC for the safety of civil aviation. The aerosol lidar system at Lauder is a two-wavelength polarization lidar. In this study, we used continuous lidar observational data observed at Lauder from 11 June through 6 July 2011.

We retrieved the backscattering ratios at 532 nm and 1064 nm and the depolarization ratio at 532 nm, and we calculated the ratio of the backscattering coefficients at 532 nm and 1064 nm. For meteorological data and derivation of the tropopause height required for the lidar data analysis, we used the twice-daily radiosonde data observed at Invercargill (46.42° S, 168.33° W), 186 km south-west of Lauder. We use the tropopause height as the lowest level at which the temperature lapse rate is less than 2 K/km for higher levels within 2 km defined by the WMO (World Meteorological Organization (WMO), 1957).

In the next section, we describe the lidar system at Lauder. In Sect. 3, we present the analysis and results and we discuss the backscatter wavelength dependence in Sect. 4.

2 Lidar system and data analysis

Lidar measurement of stratospheric aerosols at Lauder was started in November 1992, owing to interest in the then-recent eruption of Mt. Pinatubo (Uchino et al., 1995) and as a component of the nascent Network for the Detection of Stratospheric Change, subsequently the Network for the Detection of Atmospheric Composition Change. Though that system had only a single detector (532 nm), some depolarization measurements were made starting in November 1995. The system operated reliably for 17 years and recorded the decline of the Pinatubo aerosol to a minimum in the late 1990s (Nagai et al., 2010), followed by an increase in stratospheric aerosols by other volcanoes (Vernier et al., 2011; Uchino et al., 2012). In February 2009 this lidar system was updated for both daytime and night-time observations of aerosols and clouds for Greenhouse gases Observing SATellite (GOSAT) product validation (Nagai et al., 2009). The updated system is a two-wavelength polarization lidar. In this study, we use lidar data obtained by continuous measurements from 11 June 2011 to 4 July 2011, with measurements made before and after this period for GOSAT productvalidation. The main lidar specifications are summarized in Table 1. The light source of the lidar system is a Nd:YAG laser with a

second-harmonic generator: the laser thus operates at two wavelengths, 532 nm and 1064 nm. The pulse repetition rate is 10 Hz, and the transmitted energy is 150 mJ per pulse. The receiving telescope has a diameter of 30.5 cm. The signal at 1064 nm is detected with an analogue-mode avalanche photo diode (APD), and two polarization components of the signals at 532 nm are detected with three photomultiplier tubes (PMTs) from the near surface to the to a high altitude of ~ 40 km.

In this study, we used the Fernald method (Fernald, 1984), in which the lidar equation for retrieving vertical profiles of the aerosol backscatter coefficients from lidar signal intensity is solved by assuming an extinction-to-backscatter ratio (lidar ratio). We also assumed that there was no aerosol in the upper atmosphere at around 30 km, and used the value from that altitude as a reference value by which to normalize the rest of the profile. The lidar ratio is an important parameter for obtaining profiles of the particle extinction coefficient from lidar signals to use for iterative correction of the backscatter profile. The lidar ratio S is defined as the ratio of the extinction coefficient α to the backscattering coefficient β:

$$S = \frac{\alpha}{\beta}. \tag{1}$$

We assumed S to be 50 sr at both 532 and 1064 nm in this study. The lidar ratio depends on particle properties such as their size distribution and shape. The backscattering ratio R is defined as follows:

$$R = \frac{(\beta_{\mathrm{A}} + \beta_{\mathrm{M}})}{\beta_{\mathrm{M}}}, \tag{2}$$

where β_{A} is the aerosol backscattering coefficient and β_{M} is the molecular backscattering coefficient. For a pure Rayleigh atmosphere $R = 1.0$, and the backscatter signal from aerosols increases as R becomes larger than 1.0. The molecular backscattering coefficient β_{M} was calculated by using the atmospheric density profiles obtained from radiosonde data launched at Invercargill (46.45° S, 168.33° W) (Bucholtz, 1995).

The lidar transmits linearly polarized light at 532 nm and records the backscattering intensity with parallel $P_{\parallel}$ and perpendicular $P_{\perp}$ polarization to the transmitted polarization. The total

depolarization ratio δ is defined as

$$\delta = \frac{P_\perp}{(P_\perp + P_\parallel)} \times 100\,\%. \tag{3}$$

Because backscattering by spherical particles does not change the laser polarization, $\delta = 0$ for spherical particle. The depolarization ratio is sensitive to the non-spherical particles. When $\delta > 0$, the scattering by non-spherical particles is recognized (Sassen, 1991).

3 Results

3.1 Comparisons of aerosol vertical profiles before and after the eruption

Figure 1 shows the vertical profiles of R and δ before and after the PCCVC eruption. The first aerosol plume from the PCCVC eruption on 4 June 2011 was observed by lidar at Lauder at midnight on 11/12 June. The volcanic aerosol peak was located above the tropopause (10.35 km) on 11 June. The peak R value at 532 nm was 26.7 at 11.23 km, and the peak δ value at 532 nm was 16.0 % at 10.3 km. The maximum value of R on 28 May (before the eruption) around 7 km was due to tropospheric aerosols; the maximum value of R in the stratosphere was 1.09 at 16.03 km.

The integrated backscattering coefficient (IBC) is defined by Eq. (4)

$$\mathrm{IBC} = \int_{Z_{\mathrm{tr}}}^{Z_{\mathrm{top}}} \beta_{\mathrm{A}} \mathrm{d}z. \tag{4}$$

We calculated IBC from the tropopause height Z_{tr} to Z_{top}, taking $Z_{\mathrm{top}} = 30\,\mathrm{km}$. IBC represents the amount of stratospheric aerosol loading at a given location. IBC was $2.2 \times 10^{-4}\,\mathrm{sr}^{-1}$ on 28 May; this value is slightly larger than the stratospheric background value of $1.42 \times 10^{-4}\,\mathrm{sr}^{-1}$ (Nagai et al., 2010). On 11 June, after the eruption, IBC was $8.5 \times 10^{-4}\,\mathrm{sr}^{-1}$; this value indicates that the PCCVC aerosols had reached the stratosphere over Lauder. We calculated forward

trajectories to confirm that the observed profile peaks represented layers of volcanic aerosols derived from the PCCVC eruption. We calculated 10 day isentropic forward trajectories of air parcels by using the METEX (Meteorological Data Explorer) software package, which is provided by the National Institute for Environmental Studies and driven by NCEP/NCAR Reanalysis Data (Kalnay et al., 1996) 4 times daily (Fig. 2).

The initial points of 15 air parcels at 11 km altitude were located in a $1^\circ \times 1^\circ$ latitude/longitude box centered at the PCCVC eruption and released at 17:00 UTC on 4 June. The calculations showed that the air parcels leaving the volcano on 4 June 2011 reached Lauder in the early morning of 12 June. The calculations also showed that 43 % of all air parcels reached the vicinity of Lauder, and the volcanic aerosol plume from the PCCVC eruption remained near the tropopause level in the mid-latitudes of the Southern Hemisphere. These results agree with the findings of Klüser et al. (2013), who used backward trajectory calculations and observations of the Infrared Atmospheric Sounding Interferometer (IASI) on board the MetOp satellite to determine the evolution of the ash plume around the Southern Hemisphere.

3.2 Vertical profiles of the backscattering ratio and the depolarization ratio

Vertical and temporal cross sections of the backscattering ratio and depolarization ratio at 532 nm over Lauder are presented in Fig. 3. Volcanic aerosol layers with a large backscattering ratio above the tropopause heights were distinguished from the cirrus clouds present at about 8–9 km altitude, simply by the position of the tropopause except when we could calculate R at 1064 nm, because we don't have enough signal-to-noise-ratio to calculate R at 1064 nm in most of the observation period. In each ratio, we observed three peaks above the tropopause height in the analysis period, on 11 June, 23 June, and 4 July. This result suggests that the volcanic aerosol plume circled the Southern Hemisphere three times, a finding that was confirmed by using IASI, Ozone Monitoring Instrument (OMI), and Moderate Resolution Imaging Spectroradiometer (MODIS) satellite data (not shown) (Klüser et al., 2013). To examine the three peaks of the aerosol vertical profiles in greater detail, we calculated the particle depolarization

ratio δ_{p}, to estimate the non-sphericity of the particles:

$$\delta_{\mathrm{p}}(z) = \frac{\delta(z)R(z) - \delta_{\mathrm{m}}}{R(z) - 1} \times 100\,\%, \tag{5}$$

where δ is the total (molecular plus particle) depolarization ratio, calculated with Eq. (3), and δ_{m} is the depolarization ratio of atmospheric molecules. We used $\delta_{\mathrm{m}} = 0.37\,\%$ for this lidar system, defined from the spectral transmission data of the interference filter at $532\,\mathrm{nm}$ and the Rayleigh backscattering cross sections (Sakai et al., 2003). The measured δ was about 1.0-1.2 % at altitudes h igher than about 15 km (see Figs. 4(a)-(c) and 6), and this indicates that δ is sum of δ_{m} (0.37 %) and the lidar system error (about 0.65 %) where there were no aerosols. We estimated δ_{p} taking into according of this lidar system error (Sakai et al., 2003). When R is close to 1.0, δ_{p} has a lager error. For example, when $R = 1.05$ and $\delta_{\mathrm{p}} = 8$ %, the error of δ_{p} is larger than 20 %.

We estimated the proportion of non-spherical particles in the volcanic aerosol layers from the particle depolarization ratio over Lauder measured by lidar. On 11 June (Fig. 4a), the maximum values of R, δ and δ_{p} were 26.7 ($11.2\,\mathrm{km}$), 16 % ($11.8\,\mathrm{km}$) and 19 % ($12.0\,\mathrm{km}$), respectively; on 23 June (Fig. 4b), they were 18.1 ($12.0\,\mathrm{km}$), 25 % ($12.3\,\mathrm{km}$) and 32 % ($12.4\,\mathrm{km}$), respectively; and on 6 July (Fig. 4c), they were 5.3 ($11.1\,\mathrm{km}$), 20 % ($11.4\,\mathrm{km}$) and 29 % ($11.7\,\mathrm{km}$), respectively. Values of δ_{p} higher than 20 % in the aerosol layer indicate a predominance of non-spherical particles (Sakai et al., 2003). The δ_{p} values of the PCCVC volcanic aerosol layer were larger than 20 % even on the third overpass during the continuous observation period. By comparison, the δ values of the Eyjafjallajökull volcanic aerosol layers in April 2010 in Iceland were 35–40 % (Ansmann et al., 2010; Gasteiger et al., 2011). According to the analysis by Groß et al. (2012), the wavelength-independent δ_{p} values of the pure ash layer of the Eyjafjallajökull volcano were between 35 % and 38 %.

One interesting feature of the depolarization data warrants further investigation. For each of the three overpass plume observations, δ_{p} had a local minimum at the backscatter ratio peak. If this is a real physical effect and not an artifact of measurement or retrieval, it suggests some vertical separation of the volcanic plume, for which we have no ready explanation. The centroid

height of the volcanic aerosol plumes descended with time after the Pinatubo eruption (Iwasaka et al., 1995) and after the 2008 Kasatochi eruptions in the Aleutian Islands (Bitar et al., 2010). However, because our observation period was brief, we could not tell whether the height of the aerosol plumes was descending.

3.3 Aerosol optical depth derived from the backscattering ratio

Aerosol optical depth (AOD) was calculated as the product of the IBC and S. The time series of the AOD at 532 nm showed three peaks: 0.45 on 11 June, 0.31 on 23 June, and 0.12 on 5 July (Fig. 5). As discussed in Sect. 3.2, the presence of three peaks, and the decrease of the peak value with time, is an indication that the volcanic aerosol plume passed over Lauder three times.

Because the AOD as calculated in this study depends on the lidar ratio value, the appropriateness of the value chosen for that ratio needs to be considered. According to the analysis (Raman method) of Groß et al. (2012), the lidar ratio at 532 nm for the Eyjafjallajökull eruption was 49 ± 5 sr (Maisach, Germany), and according to the analysis of Ansmann et al. (2010), it ranged from 55 ± 5 sr (Maisach) to 60 ± 5 sr (Leipzig, Germany). Hoffmann et al. (2010) reported that the lidar ratio at 532 nm for the Kasatochi eruption event was 65 ± 10 sr. We compared the AODs reported above with AODs calculated by a method that does not use the lidar ratio (Uchino et al., 1983). In this method, the transmission $\tau(z_1, z_2)$, between altitude z_1 and z_2 is

$$\tau(z_1, z_2) = \frac{z_2}{z_1} \left[\frac{p(z_2) R(z_1) \beta_{\mathrm{m}}(z_1)}{p(z_1) R(z_2) \beta_{\mathrm{m}}(z_2)} \right]^{1/2}, \tag{6}$$

where $p(z)$ is the total received signal photon count at altitude z, $\beta_{\mathrm{m}}(z)$ is the atmospheric molecular backscattering coefficient, and $R(z)$ is the backscattering ratio. The transmission can be determined by choosing two altitudes, z_1 and z_2, where no aerosols are assumed to exist; therefore, $R(z_1) = R(z_2) = 1.0$. For example, the AOD on 11 June as determined by this method was 0.52 ± 0.08 ($z_1 = 8.4$ km and $z_2 = 12.0$ km); this AOD value is 13 % larger than the AOD derived from the IBC and S. The values of AOD derived by Eq. (6) are 0.17 and 0.12 on 24 June and 6 June, respectively. On average, the AOD derived by IBC was about 20 % smaller

than AOD derived by Eq. (6). If the lidar ratio is assumed to be 60 sr, AOD will be consistent each other.

4 Discussion

The observed PCCVC particle depolarization ratios δ_{p} were large. On 11 June, the maximum δ_{p} was 23 %; on 23 June, it was 33 %; and on 6 July, it was 29 %. These large values indicate that the aerosol particles were non-spherical. We then calculated the backscatter-related wavelength exponent A_β as follows:

$$A_\beta = -\frac{\ln(\beta_{532}/\beta_{1064})}{\ln(532/1064)}, \tag{7}$$

where β_{532} and β_{1064} are the backscattering coefficients at 532 nm and 1064 nm. A_β provides information about the size distribution of both spherical and non-spherical particles that takes account of the complex dependence of backscatter on particle component size, wavelength, and non-sphericity. $A_\beta > 2$ indicates relatively smaller particles (radius $\leq 0.5\,\mu\mathrm{m}$) and A_β around zero indicates larger particles (radius $\geq 0.5\,\mu\mathrm{m}$) (Kaufman et al., 1994; Schuster et al., 2006). For background stratospheric aerosols, A_β is about 2.0 (Shibata et al., 1984; Hofmann et al., 2009); for cloud layers A_β is about -0.2 to 0.0 (Kamei et al., 2006; Mona et al., 2012), and for volcanic ash A_β is about 1.0 (Ansmann et al., 2012).

Figure 6a displays the vertical profiles of R, δ and δ_{p} at 532 nm, and Fig. 6b shows the vertical profiles of R at 532 nm and1064 nm and of A_β at 532 nm/1064 nm, on 13 June. The peak of R was below the tropopause, but we infer that this represents the volcanic layer because its average A_β at 11–13 km altitude was 0.92, whereas that of the stratospheric background aerosols at 13–15 km was 2.54, and the mean value of cirrus clouds at 8–9.5 km was 1.29×10^{-2}. Although the stratospheric aerosol A_β value at 13–15 km is a little larger than the literature value, the A_β values of the volcanic aerosols and cirrus clouds are consistent with value reported by previous studies (Kamei et al., 2006; Mona et al., 2012; Ansmann et al., 2012). This result indicates that it should be possible to distinguish between a volcanic aerosol layer and underlying cirrus

clouds by using the vertical profile of A_β. Unfortunately, because there were optically thick clouds under the volcanic aerosol layers and the vertical backscattering coefficient at 1064 nm were very noisy, we were not able to apply this method to distinguish the aerosols and cirrus clouds on the other days.

It is possible to use A_β, δ and δ_p derived from lidar measurement to determine approximately the proportions of sulfur acid aerosols and the ash particles. However, it is not possible to determine the absolute quantity of these particles. Typically, non-spherical and larger particles are volcanic ash, whereas spherical and smaller particles are sulfuric acid aerosols. As mentioned in Sect. 3, the finding that the total and particle depolarization ratios of the PCCVC volcanic aerosols were larger than 20 % suggests that the volcanic plume included many non-spherical and large particles. Therefore, we concluded that the dominant component of the plume observed over Lauder was volcanic ash.

Similarly, for aerosols from the eruption of Eyjafjallajökull, the total depolarization ratios were 35–40 % (Ansmann et al., 2010; Gasteiger et al., 2011). In contrast, the Kasatochi ratios were 1.5–5.0 % (Hoffmann et al., 2010) and the ratios for aerosols from the eruption of Nabro volcano in Eritrea in 2011 were $\delta = 1$–2 % and $\delta_\mathrm{p} = 4$–7 % (Uchino et al., 2012). In the case of the eruption of Eyjafjallajökull, Ansmann et al. (2011) reported that sulfate aerosols originating from volcanic SO_2 plumes contributed about 50 % of the particle mass. Miffre et al. (2011) used the volcanic ash particle depolarization ratio $\delta = 40 \pm 0.2$ % obtained from laboratory measurements performed by Muñoz et al. (2004) to determine the composition of the Eyjafjallajökull plume.

Recent studies have provided estimates of SO_2 emission from several eruption events. Karagulian et al. (2010) estimated the total mass of SO_2 ejected by the Kasatochi eruption to be 1.7 Tg, based on the IASI high-spectral-resolution infrared radiance measurements. Haywood et al. (2010) estimated that 1.2 Tg of SO_2 was ejected by the Sarychev (Kuril Islands) eruption in June 2009. Clarisse et al. (2012), using IASI data, reported that 1.5 Tg of SO_2 was ejected by the Nabro volcano, and 0.25 Tg by the PCCVC eruption. Because less SO_2 was ejected by the eruption of Puyehue-Cordón Caulle compared with the amounts ejected by the eruptions of

Nabro and Kasatochi, the tephra fraction of the PCCVC plume was greater, and its depolarization ratios were larger.

We next estimated the influence of the PCCVC volcanic ash particles on the column averaged dry air mole fraction of carbon dioxide (XCO_2) determined by GOSAT. When the GOSAT XCO_2 is retrieved by using the 1.6 µm band without taking account of volcanic ash particles in the upper troposphere and lower stratosphere, the negative bias of XCO_2 is estimated to be 2 % for an AOT of 0.4 at 532 nm and surface albedo of 0.2 at Lauder 0.28 (based on MODIS band2).

5 Summary

On 4 June 2011, the Puyehue-Cordón Caulle Volcanic Complex (40.59° S, 72.11° W) in Chile erupted and the volcanic plume passed over Lauder in New Zealand. Because the VAAC at Wellington had forecast that the aerosol plume would pass over New Zealand, we started continuous lidar observations on 11 June. On the same day, we detected the PCCVC volcanic aerosol layer from the profiles of the backscattering ratio R and the depolarization ratio δ at 532 nm. This observational result was confirmed by a forward trajectory analysis done by using METEX and some satellite data (from the MODIS, OMI and IASI instruments). We found that the volcanic aerosol layer peak passed over Lauder three times from 11 June to 6 July at intervals of 10–12 days. The maximum R value on 11 June, immediately after the eruption, was 27 at 11.2 km, and the AOD was 0.45. This R value is much larger than the maximum R value of 2.0–3.5 observed at Saga and Tsukuba, Japan, for the Nabro volcano, which erupted on 12 June 2011 Uchino et al. (2012). On 11 June, when the continuous lidar observation started, the maximum value of δ was 16 % and that of δ_{p} was 23 %. On 6 July, at the end of the period of continuous lidar observations, the maximum value of δ was 20 %, and that of δ_{p} was 29 %. Thus, δ_{p} remained at 20–30 % over the entire observation period, and even one month after the eruption the depolarization ratio had not decreased. This result indicates that the major component of the PCCVC volcanic aerosol layers was non-spherical particles.

The backscatter-related wavelength exponent of the PCCVC volcanic aerosols at 1064/532 nm was 0.9 at 11–13 km altitude; this value indicates that the PCCVC volcanic aerosols were composed of large particles. According to Ansmann et al. (2012), the wavelength exponents of the Eyjafjallajökull volcanic aerosols were 1.12–1.19. The wavelength exponents of the Kasatochi eruption aerosols were 0.5–1.5 (Tesche et al., 2010). The lidar observations at Lauder showed that the PCCVC volcanic aerosol layers contained non-spherical and larger particles. These results agree with the findings of previous studies, which reported that the volcanic plume of the PCCVC eruption contained less SO_2 than the plumes from the Kasatochi and Nabro eruptions (Karagulian et al., 2010; Clarisse et al., 2012).

Supplementary material related to this article is available online at: http://\@journalurl/\@pvol/\@fpage/\@pyear/\@journalnameshortlower-\@pvol-\@fpage-\@pyear-supplement.zip.

Acknowledgements. This research was supported in part by the Environment Research and Technology Development Fund (2A-1102) of the Ministry of the Environment, Japan. The author wish to thank the editor.

References

Alados-Arboledas, L., Olmo, F. J., Ohvril, H. O., Teral, H., Arak, M., and Teral, K.: Evolution of solar radiative effects of Mount Pinatubo at ground level, Tellus-B, 49, 2, 190–198, 1997.

Ansmann, A., Tesche, M., Grofl, S., Freudenthaler, V., Seifert, P., Hiebsch, A., Schmidt, J., Wandinger, U., Mattis, I., Müller, D., and Wiegner, M.: The 16 April 2010 major volcanic ash plume over central Europe: EARLINET lidar and AERONET photometer observations at Leipzig and Munich, Germany, Geophys. Res. Lett., 37, L13 810, doi:http://dx.doi.org/10.1029/2010GL04380910.1029/2010GL043809, 2010.

Ansmann, A., Tesche, M., Seifert, P., Groß, S., Freudenthaler, V., Apituley, A., Wilson, K. M., Serikov, I., Linnú, H., Heinold, B., Hiebsch, A., Schnell, F., Schmidt, J., Mattis, I., Wandinger, U., and Wiegner,

M.: Ash and fine-mode particle mass profiles from EARLINET-AERONET observations over central Europe after the eruptions of the Eyjafjallajökull volcano in 2010, J. Geophys. Res., 116, D00U02, doi:http://dx.doi.org/10.1029/2010JD01556710.1029/2010JD015567, 2011.

Ansmann, A., Seifert, P., Tesche, M., and Wandinger, U.: Profiling of fine and coarse particle mass: case studies of Saharan dust and Eyjafjallajökull/Grimsvötn volcanic plumes, Atmos. Chem. Phys., 12, 9399–9415, doi:http://dx.doi.org/10.5194/acp-12-9399-201210.5194/acp-12-9399-2012, 2012.

Bernard, A. and Rose, W. I.: The injection of sulfuric acid aerosols in the stratosphere by El Chichon Volcano and its related hazards to the international air traffic, Natural Hazards, 3, 59–67, 1990.

Bitar, L., Duck, T. J., Kristiansen, N. I., Stohl, A., and Beauchamp, S.: Lidar observations of Kasatochi volcano aerosols in the troposphere and stratosphere, J. Geophys. Res., 115, D00L13, doi:http://dx.doi.org/10.1029/2009JD01365010.1029/2009JD013650, 2010.

Bluth, G. J. S., Doiron, S. D., Schnetzler, S. C., Krueger, A. J., and Walter, L. S.: Global tracking of the SO_2 clouds from the June 1991 Mount Pinatubo eruptions, Geophys.Res.Lett., 19, 151–154, 1992.

Bucholtz, A.: Rayleigh-scattering calculations for the terrestrial atmosphere, Appl. Opt., 34, 15, 2765–2773, 1995.

Clarisse, L., Hurtmans, D., Clerbaux, C., Hadji-Lazaro, J., Ngadi, Y., and Coheur, P.-F.: Retrieval of sulphur dioxide from the infrared atmospheric sounding interferometer (IASI), Atmos. Meas. Tech., 5, 581–594, doi:http://dx.doi.org/10.5194/amt-5-581-201210.5194/amt-5-581-2012, 2012.

Deshler, T.: A review of global stratospheric aerosol: Measurements, importance, life cycle, and stratospheric aerosol, J. Atmos. Res., D90, 223–232, doi:http://dx.doi.org/10.1016/j.atmosres.2008.03.01610.1016/j.atmosres.2008.03.016, 2008.

Durant, A. J., Shaw, R. A., Rose, W. I., Mi, Y., and Ernst, G. G. J.: Ice nucleation and overseeding of ice in volcanic clouds, J. Geophys. Res., 113, D09 206, doi:http://dx.doi.org/10.1029/2007JD00906410.1029/2007JD009064, 2008.

Dzierma, Y. and Wehrmann, H.: On the likelihood of future eruptions in the Chilean Southern Volcanic Zone: interpreting the past century ’s eruption record based on statistical analyses, Andean Geology, 39, 3, 380–393, doi:http://dx.doi.org/10.5027/andgeoV39n3-a0210.5027/andgeoV39n3-a02, 2012.

Fernald, F. G.: Analysis of atmospheric lidar observations: some comments, Appl. Opt., 23, 5, 652–653, 1984.

Gasteiger, J., Groß, S., Freudenthaler, V., and Wiegner, M.: Volcanic ash from Iceland over Munich: Mass concentration retrieved from ground-based remote sensing measurements, Atmos. Chem. Phys., 11, 2209–2223, doi:http://dx.doi.org/10.5194/acp-11-2209-201110.5194/acp-11-2209-2011, 2011.

Groß, S., Freudenthaler, V., Wiegner, M., Gasteiger, J., Geiß, A., and Schnell, F.: Dual-wavelength linear depolarization ratio of volcanic aerosols: Lidar measurements of the Eyjafjallajökull plume over Maisach, Germany, Atmos. Environ., 48, 85–96, doi:http://dx.doi.org/10.1016/j.atmosenv.2011.06.01710.1016/j.atmosenv.2011.06.017, 2012.

Haywood, J. M., Jones, A., Clarisse, L., Bourassa, A., Barnes, J., Telford, P., Bellouin, N., Boucher, O., Agnew, P., Clerbaux, C., Coheur, P., Degenstein, D., and Braesicke, P.: Observations of the eruption of the Sarychev volcano and simulations using the HadGEM2 climate model, J. Geophys. Res., 115, D21 212, doi:http://dx.doi.org/10.1029/2010JD01444710.1029/2010JD014447, 2010.

Hoffmann, A., Ritter, C., Stock, M., Maturilli, M., Eckhardt, S., Herber, A., and Neuber, R.: Lidar measurements of the Kasatochi aerosol plume in August and September 2008 in Ny-Alesund, Spitsbergen, J. Geophys. Res., 115, D00L12, doi:http://dx.doi.org/0.1029/2009JD0130390.1029/2009JD013039, 2010.

Hofmann, D., Barnes, J., O'Neill, M., Trudeau, M., and Neely, R.: Increase in background stratospheric aerosol observed with lidar at Mauna Loa Observatory and Boulder, Colorado, Geophys. Res. Lett., 36, L15 808, doi:http://dx.doi.org/10.1029/2009GL03900810.1029/2009GL039008, 2009.

Iwasaka, Y., Shibata, T., Hayashi, M., Nagatani, M., Ojio, T., Adachi, H., Matsunaga, K., Osada, K., Mori, I., Fujiwara, M., Akiyoshi, E., Shiraishi, K., Yamazaki, K., Kondoh, K., and Nakane, H.: Lidar Measurements at Alaska, 1991-1994. Pinatubo Volcanic Effect on Stratospheric Aerosol Layer, The Review of Laser Engineering, 23, 2, 166–170, 1995.

Kalnay, E., Kanamitsu, M., Kistler, R., Collins, W., Deaven, D., Gandin, L., Iredell, M., Saha, S., White, G., Woollen, J., Zhu, Y., Leetmaa, A., Reynolds, R., Chelliah, M., Ebisuzaki, W., Higgins, W., Janowiak, J., Mo, K. C., Ropelewski, C., Wang, J., Jenne, R., and Joseph, D.: The NCEP/NCAR 40-Year Reanalysis Project, Bull. Amer. Meteor. Soc., 77, 3, 437–471, 1996.

Kamei, A., Sugimoto, N., Matsui, I., Shimizu, A., and Shibata, T.: Volcanic aerosol layer observed by shipboard lidar over the tropical western Pacific, SOLA, 2, 1–4, doi:http://dx.doi.org/10.2151/sola.2006-00110.2151/sola.2006-001, 2006.

Karagulian, F., Clarisse, L., Clerbaux, C., Prata, A. J., Hurtmans, D., and Coheur, P. F.: Detection of volcanic SO_2, ash, and H_2SO_4 using the Infrared Atmospheric Sounding Interferometer, J. Geophys. Res., 115, D00L02, doi:http://dx.doi.org/10.1029/2009JD01278610.1029/2009JD012786, 2010.

Kaufman, Y. J., Gitelson, A., Karnieli, A., Ganor, E., Fraser, R. S., Nakajima, T., Mattoo, S., and Holben, B. N.: Size distribution and scattering phase function of aerosol particles retrieved from sky brightness measurements, J. Geophys. Res., 99, D5, 10 341—10 356, doi:http://dx.doi.org/10.1029/94JD0022910.1029/94JD00229, 1994.

Klüser, L., Erbertseder, T., and Meyer-Arnek, J.: Observation of volcanic ash from Puyehue Cordón Caulle with IASI, Atmos. Meas. Tech., 6, 35–46, doi:http://dx.doi.org/10.5194/amt-6-35-201310.5194/amt-6-35-2013, 2013.

Lara, L. E., Moreno-Roa, H., and Naranjo, J. A.: Rhyodacitic fissure eruption in Southern Andes (Cordón Caulle; 40.5°S) after the 1960 (Mw:9.5) Chilean earthquake: A structural interpretation, J. Volcanol. Geoth. Res., 138, 127–138, doi:http://dx.doi.org/10.1016/j.jvolgeores.2004.06.00910.1016/j.jvolgeores.2004.06.009, 2004.

Lathem, T. L., Kumar, P., Nenes, A., Dufek, J., Sokolik, I. N., Trail, M., and Russell, A.: Hygroscopic properties of volcanic ash, Geophys. Res. Lett., 38, 11, L11 802, doi:http://dx.doi.org/10.1029/2011GL04729810.1029/2011GL047298, 2011.

McCormick, M. P., Thomason, L. W., and Trepte, C. R.: Atmospheric effects of the Mt Pinatubo eruption, Nature, 373, 399–404, doi:http://dx.doi.org/10.1038/373399a010.1038/373399a0, 1995.

Miffre, A., David, G., Thomas, B., Abou-Chacra, M., and Rairoux, P.: Interpretation of Accurate UV Polarization Lidar Measurements: Application to Volcanic Ash Number Concentration Retrieval, J. Atmos. Oceanic Technol., 29, 558–568, doi:http://dx.doi.org/10.1175/JTECH-D-11-00124.110.1175/JTECH-D-11-00124.1, 2011.

Minnis, P., Harrison, E. F., Stowe, L. L., Gison, G. G., M.Denn, F., Doelling, D. R., and Smith, W. L. J.: Radiative climate forcing by the Mount Pinatubo eruption, Science, 259, 1411–1415, 1993.

Mona, L., Amodeo, A., D'Amico, G., Giunta, A., Madonna, F., and Pappalardo, G.: Multi-wavelength Raman lidar observations of the Eyjafjallajökull volcanic cloud over Potenza, Southern Italy, Atmos. Chem. Phys., 12, 2229–2244, doi:http://dx.doi.org/10.5194/acp-12-2229-201210.5194/acp-12-2229-2012, 2012.

Muñoz, O., Volten, H., Hovenier, J. W., Veihelmann, B., van der Zande, W. J., Waters, L. B. F. M., and Rose, W. I.: Scattering matrices of volcanic ash particles of Mount St. Helens, Redoubt, and Mount Spurr Volcanoes, J. Geophys. Res., 109, D16 201, doi:http://dx.doi.org/10.1029/2004JD00468410.1029/2004JD004684, 2004.

Nagai, T., Sakai, T., Uchino, O., Morino, I., Yokota, T., and Liley, B., eds.: Lidar observations of clouds and aerosols over Lauder in the Southern Hemisphere for GOSAT validation, Proceeding of the 46th spring conference of the Remote Sensing Society of Japan, 2009.

Nagai, T., Liley, B., Sakai, T., Shibata, T., and Uchino, O.: Post-Pinatubo Evolution and Subsequent Trend of the Stratospheric Aerosol Layer Observed by Mid-Latitude Lidars in Both Hemispheres, SOLA, 6, 69–72, doi:http://dx.doi.org/10.2151/sola.2010-01810.2151/sola.2010-018, 2010.

Newhall, C. G. and Self, S.: The volcanic explosivity index (VEI) an estimate of explosive magnitude for historical volcanism, J. Geophys. Res., 87, C2, doi:http://dx.doi.org/10.1029/JC087iC02p0123110.1029/JC087iC02p01231, 1982.

Raga, G. B., Baumgardner, D., Ulke, A. G., Brizuela, M. T., and Kucienska, B.: The environmental impact of the Puyehue-Cordón Caulle 2011 volcanic eruption on Buenos Aires, Nat. Hazards Earth Syst. Sci., 13, 2319–2330, doi:http://dx.doi.org/10.5194/nhess-13-2319-201310.5194/nhess-13-2319-2013, 2013.

Robock, A.: Volcanic eruptions and climate, Rev. Geophys., 38, 191–219, doi:http://dx.doi.org/10.1029/1998RG00005410.1029/1998RG000054, 2000.

Sakai, T., Nagai, T., Nakazato, M., Mano, Y., and Matsumura, T.: Ice clouds and Asian dust studied with lidar measurements of particle extinction-to-backscatter ratio, particle depolarization, and water-vapor mixing ratio over Tsukuba, Appl. Opt., 42, 36, 7103–7116, 2003.

Sassen, K.: The polarization lidar technique for cloud research: A review and cu rrent assessment, Bull. Amer. Meteor. Soc., 72, 1848–1866, 1991.

Schuster, G. L., Dubovik, O., and Holben, B. N.: Angstrom exponent and bimodal aerosol size distributions, J. Geophys. Res, 111, D07 207, doi:http://dx.doi.org/10.1029/2005JD00632810.1029/2005JD006328, 2006.

Shibata, T., Fujiwara, M., and Hirono, M.: The El Chichon volcanic cloud in the stratosphere: lidar observation at Fukuoka and numerical simulation, J. Atmos. Terr. Phys., 46, 12, 1121–1146, 1984.

Solomon, S., Daniel, J. S., Neely, R. R., Vernier, J.-P., Dutton, E. G., and Thomaso, L. W.: The Persistently Variable "Background" Stratospheric Aerosol Layer and Global Climate Change, Science, 33, 866–870, doi:http://dx.doi.org/10.1126/science.120602710.1126/science.1206027, 2011.

Tesche, M., Ansmann, A., Hiebsch, A., Mattis, I., Schmidt, J., Seifert, P., and Wandinger, U.: Lidar observations of the Eyjafjallajökull volcanic ash plume at Leipzig, Germany, Proc. SPIE, 7832, 78 320L–1, doi:http://dx.doi.org/10.1117/12.86851610.1117/12.868516, 2010.

Trickl, T., Giehl, H., Jäger, H., and Vogelmann, H.: 35 yr of stratospheric aerosol measurements at Garmisch-Partenkirchen: from Fuego to Eyjafjallajökull, and beyond, Atmos. Chem. Phys., 13, 5205–5225, doi:http://dx.doi.org/10.5194/acp-13-5205-201310.5194/acp-13-5205-2013, 2013.

Uchino, O., Tokunaga, M., Seki, K., Maeda, M., Naito, K., and Takahashi, K.: Lidar measurement of stratospheric transmission at a wavelength of 340 nm after the eruption of El Chichon, J. Atmos. Terr. Phys., 45, 12, 849–850, 1983.

Uchino, O., Nagai, T., Fujimoto, T., Matthews, W. A., and Orange, J.: Extensive lidar observations of the Pinatubo aerosol layers at Tsukuba (36.1°N), Naha

(26.2°N), Japan and Lauder (45.0°S), New Zealand, Geophys. Res. Lett., 22, 57–60, doi:http://dx.doi.org/10.1029/94GL0273510.1029/94GL02735, 1995.

Uchino, O., Sakai, T., Nagai, T., Nakamae, K., Morino, I., Arai, K., Okumura, H., Takubo, S., Kawasaki, T., Mano, Y., Matsunaga, T., and Yokota, T.: On recent (2008–2012) stratospheric aerosols observed by lidar over Japan, Atmos. Chem. Phys., 12, 11 975–11 984, doi:http://dx.doi.org/10.5194/acp-12-11975-201210.5194/acp-12-11975-2012, 2012.

Vernier, J.-P., Thomason, L. W., Pommereau, J.-P., Bourassa, A., Pelon, J., Garnier, A., Hauchecorne, A., Blanot, L., Trepte, C., Degenstein, D., and Vargas, F.: Major influence of tropical volcanic eruptions on the stratospheric aerosol layer during the last decade, Geophys. Res. Lett., 38, 12, L12 807, doi:http://dx.doi.org/10.1029/2011GL04756310.1029/2011GL047563, 2011.

Wiegner, M., Gasteiger, J., Groß, S., Schnell, F., Freudenthaler, V., and Forkel, R.: Characterization of the Eyjafjallajökull ash-plume: potential of lidar remote sensing, J. Phys. Chem. Earth, 45-46, 79–86, 2012.

World Meteorological Organization (WMO): Definition of the tropopause, WMO Bull., 6, 136, 1957.

Wu, P.-M., Okada, K., Tanaka, T., Sasaki, T., Nagai, T., Fujimoto, T., and Uchino, O.: Balloon observation of stratospheric aerosols over Tsukuba, Japan Two years after the Pinatubo volcanic eruption, J. Meteor. Soc. Jpn., 72, 475–480, 1994.

Zhao, J., Turco, R. P., and Owen, O. B.: A model simulation of Pinatubo volcanic aerosols in the stratosphere, J. Geophys. Res., 100, D4, 7315–7328, doi:http://dx.doi.org/10.1029/94JD0332510.1029/94JD03325, 1995.

Table 1. Lidar system at Lauder, New Zealand.

System after update (after 18 Feb 2009)		
Transmitter		
Laser	Nd:Yag	
Wavelength	532 nm	1064 nm
Pulse Energy	150 mJ	150 mJ
Pulse Repetition	10 Hz	
Beam Divergence	0.2 mrad	
Receiver		
Telescope Type	Ritchey–Chrétien (advanced)	
Wavelength	532 nm	1064 nm
Telescope Diameter	30.5 cm (12 inch)	
Field of View (full angle)	1.0 mrad	
Band Width (FWHM)	0.28 nm	0.34 nm
Polarization measurement	Yes	No
Number of Receiving Channel	3	1
Detector	PMT	APD
Signal Processing	12 bit A/D + Photon counting	12 bit A/D
Time Resolution	10 s (max), 5 min (nominal)	
Altitude Resolution	7.5 m	

Fig. 1. Vertical profiles of backscattering (left) and depolarization (right) ratios before (28 May, blue line) and after (11 June, red line) the PCCVC eruption on 4 June 2011. The horizontal dot-dash line in each panel shows the tropopause height derived from radiosonde data at Invercargill.

Fig. 2. Ten-day isentropic forward trajectories of air parcels (colored lines) determined by using METEX. The starting position was the PCCVC (40.59° S, 72.11° W), at 11 km above the surface. Large black dots mark each 24 h period in the simulation.

Fig. 3. Vertical and temporal cross-section of the backscattering ratio **(a)** and the depolarization ratio **(b)** at 532 nm. The light purple rectangles show tropopause height.

Fig. 4. Vertical profiles of the backscattering ratio R (blue line), the total depolarization ratio δ (red line) and the particle depolarization ratio δ_{p} (green line) observed at on **(a)** 11 June at 18:00 LT, **(b)** 23 June at 18:00 LT, and **(c)** 6 July at 03:00 LT. The horizontal dot-dash lines in each panel shows tropopause height; **(a)** 10.3 km, **(b)** 10.6 km and **(c)** 9.4 km. The volcanic aerosol layers are indicated by the R, δ and δ_{p} peaks above the tropopause height. The error bars are also show for R, δ, and δ_{p} profiles.

Fig. 5. Temporal variation of the stratospheric AOD over Lauder from 11 June to 6 July 2011. Three AOD peaks occurred of 0.45 on 11 June, 0.31 on 23 June and 0.12 on 6 July.

Fig. 6. (a) Vertical profiles of the backscattering ratio R (blue line), the total depolarization ratio δ (red line), and the particle depolarization ratio δ_{p} (green line) at 532 nm on 13 June. The horizontal dot-dash lines in each panel shows tropopause height. **(b)** Vertical profiles of the backscattering ratio at 532 nm (blue line), the backscattering ratio at 1064 nm (orange line), and the wavelength exponent of the backscattering ratios (A_β) at 1064 nm/532 nm (red line) on 13 June.

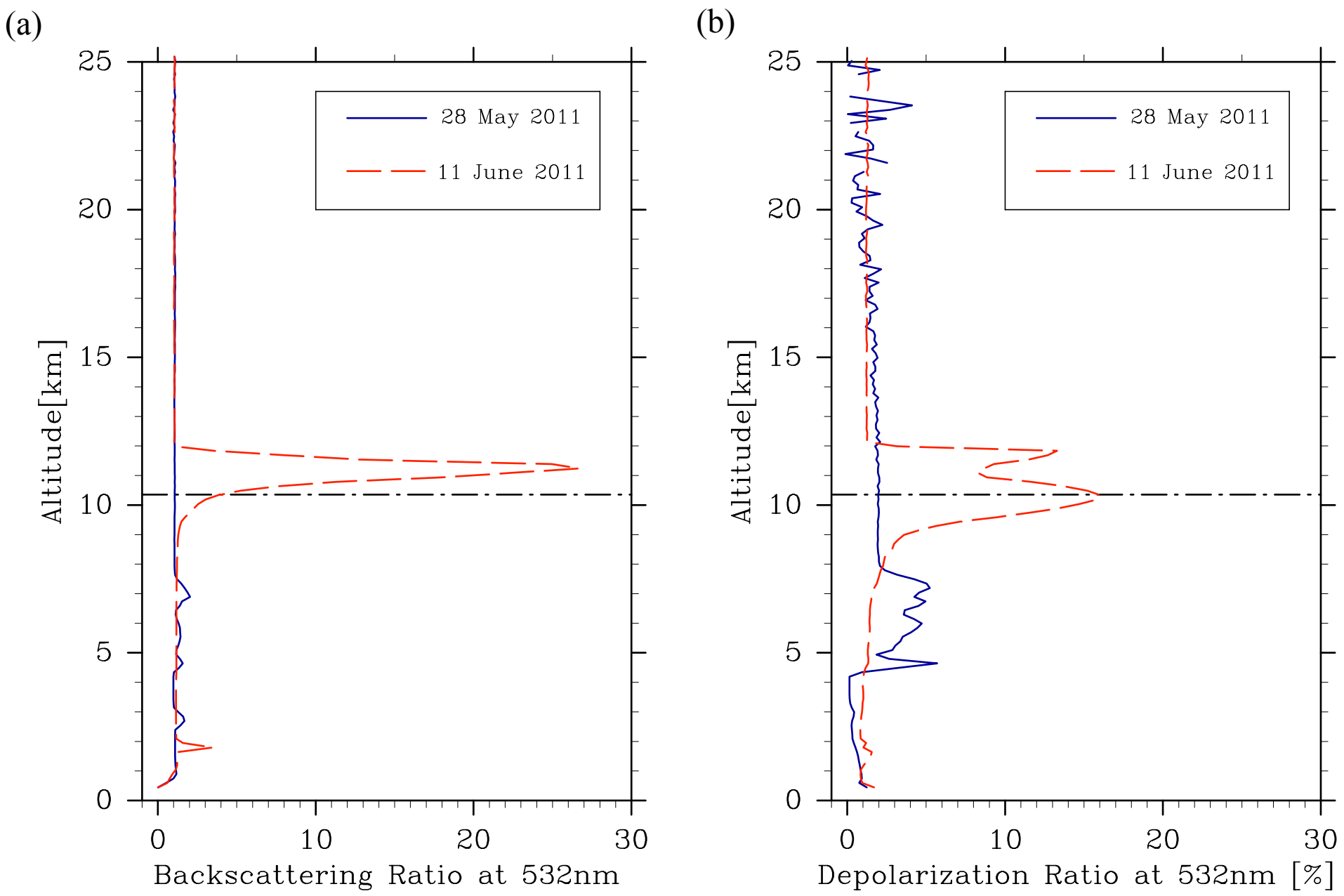
(a)
(b)
28 May 2011
11 June 2011
Altitude[km]
Backscattering Ratio at 532nm
Depolarization Ratio at 532nm [%]
0
5
10
15
20
25
0
10
20
30

Fig. 1

(a)

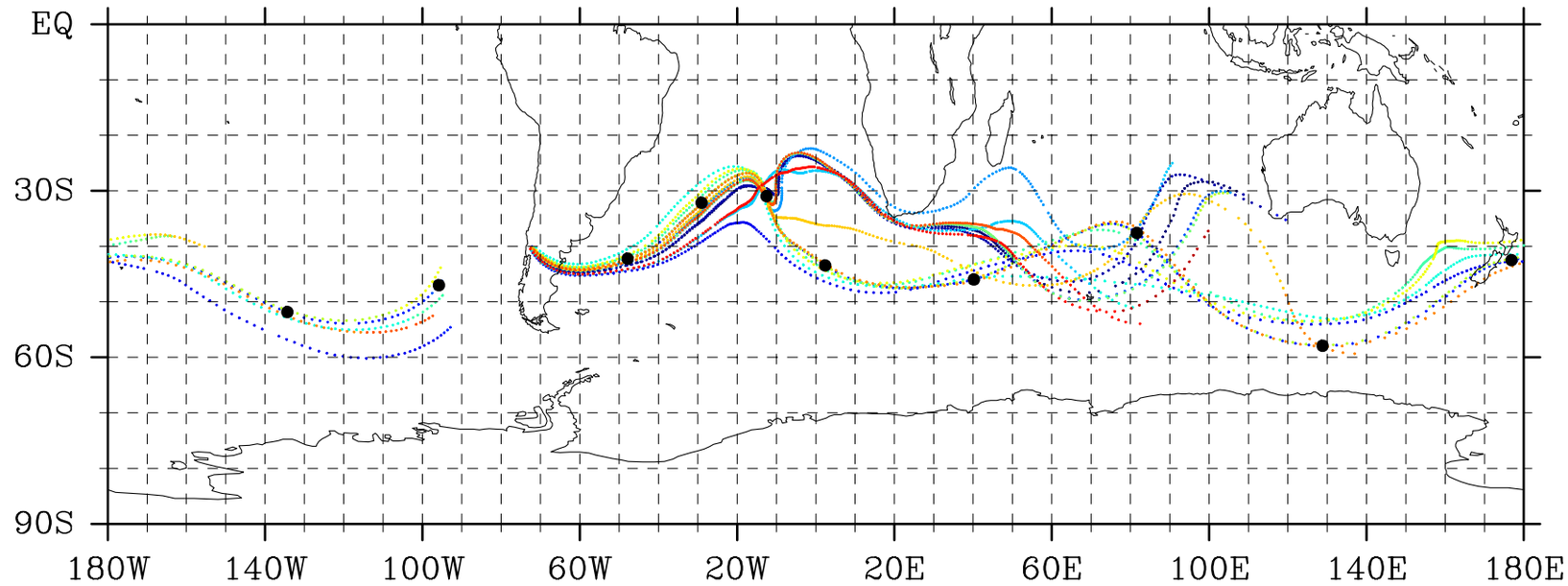
EQ
30S
60S
90S
180W
140W
100W
60W
20W
20E
60E
100E
140E
180E

(b)

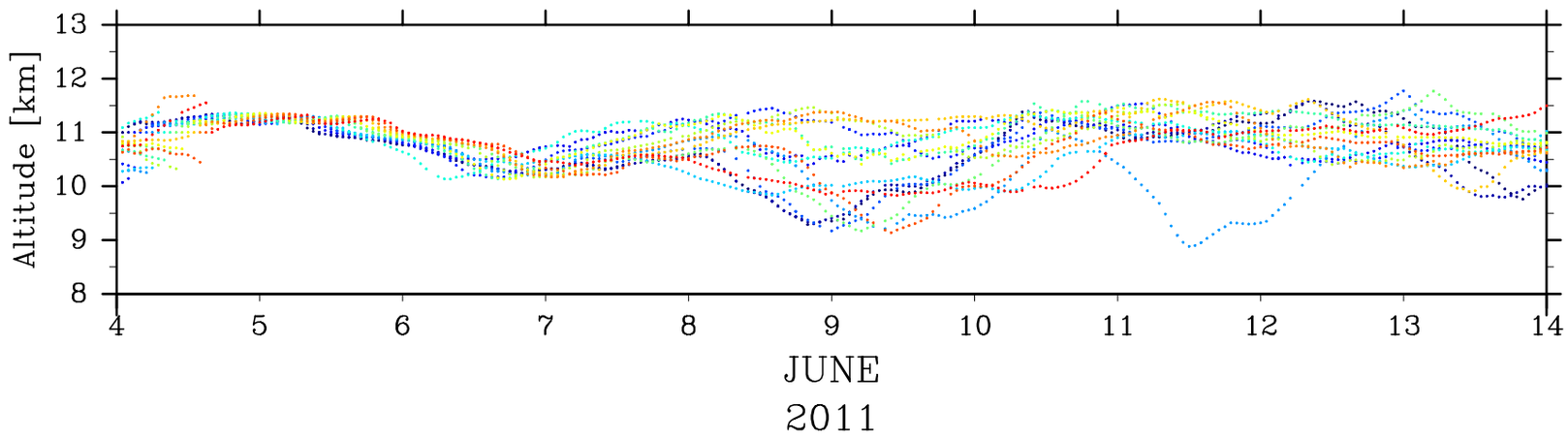
Altitude [km]
13
12
11
10
9
8
4
5
6
7
8
9
10
11
12
13
14
JUNE
2011

Fig.2

(a)

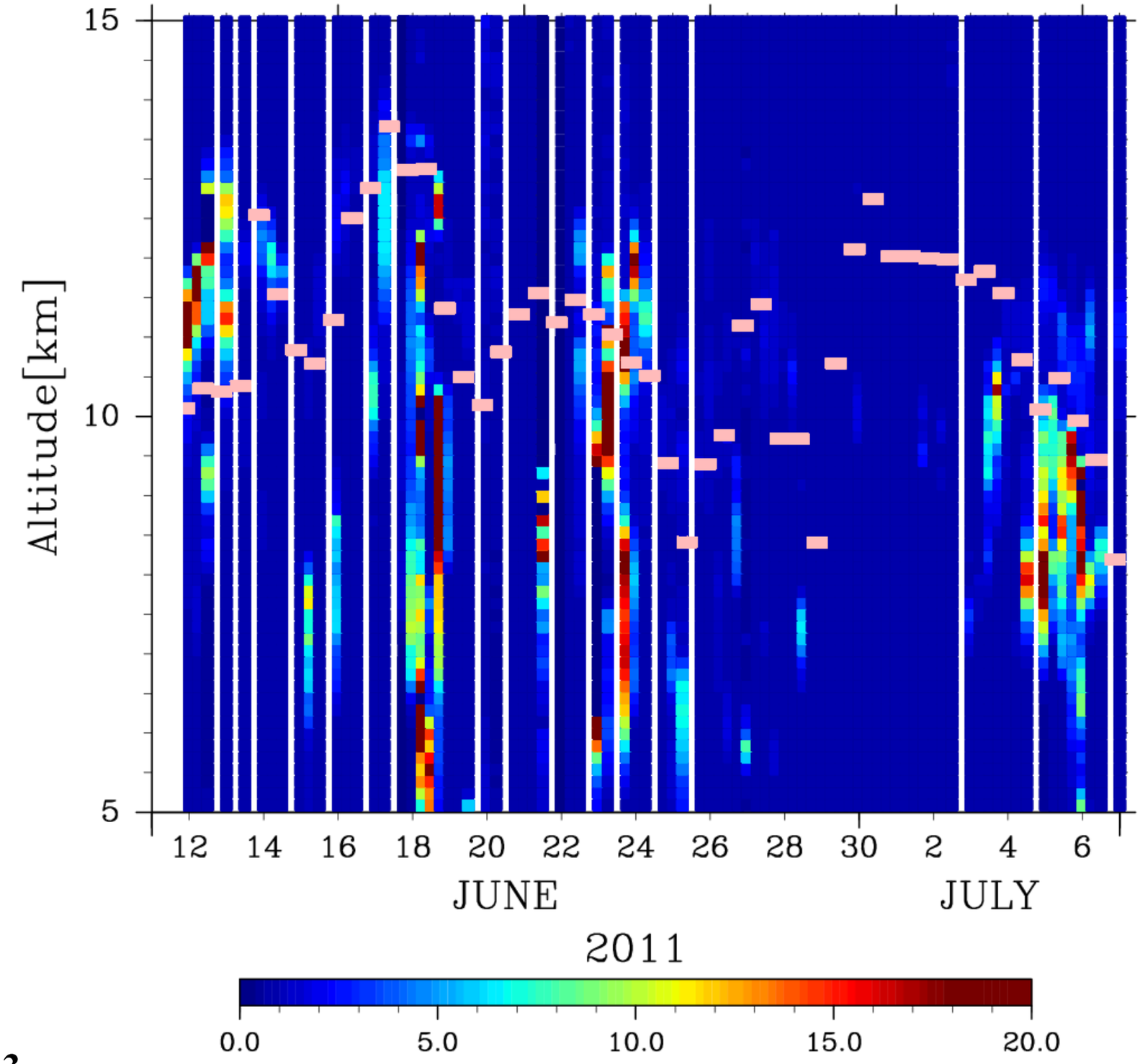
15
10
5
Altitude[km]
12
14
16
18
20
22
24
26
28
30
2
4
6
JUNE
JULY
2011
0.0
5.0
10.0
15.0
20.0

Fig.3

(b)

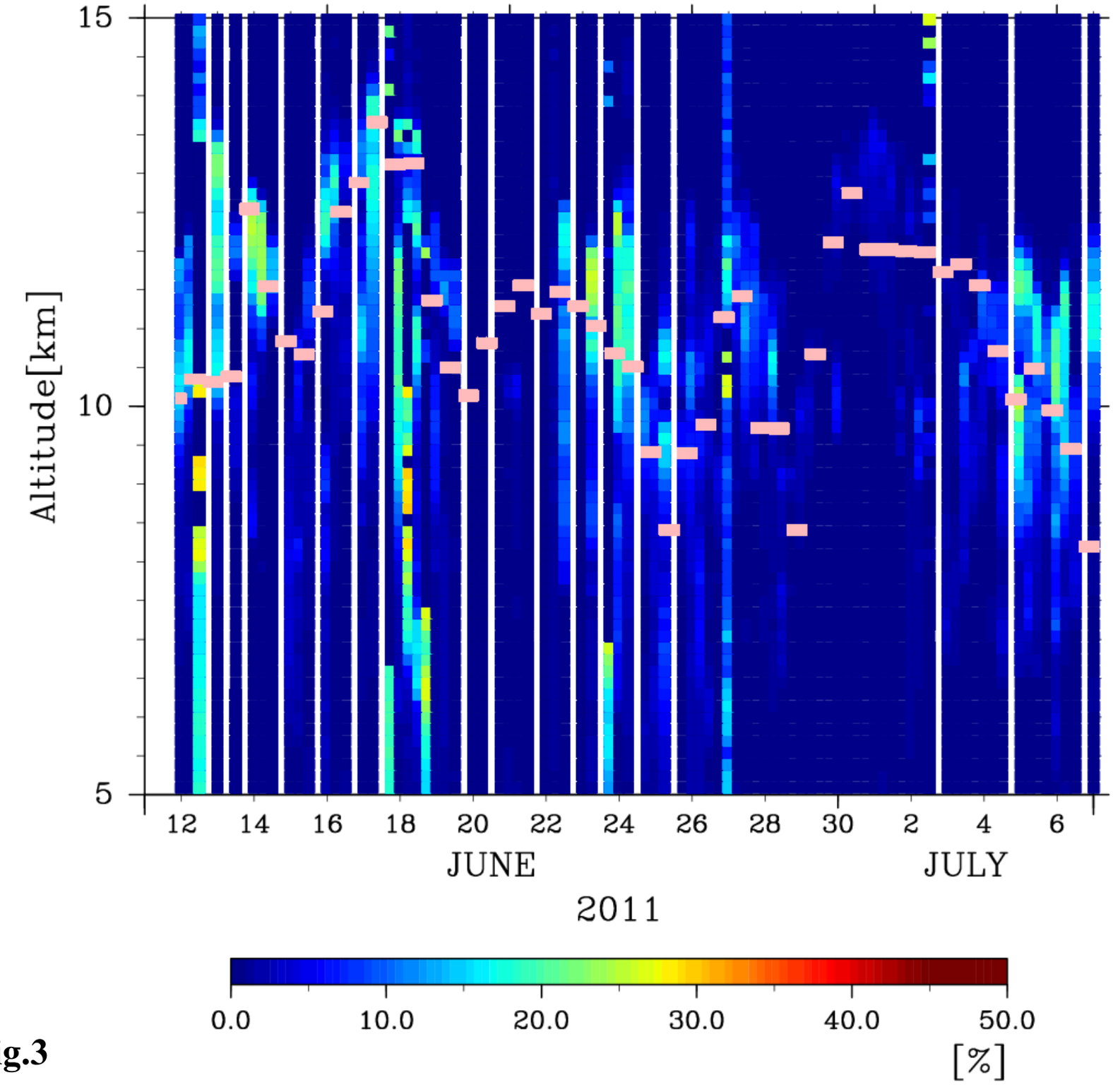
15
10
5
Altitude[km]
12
14
16
18
20
22
24
26
28
30
2
4
6
JUNE
JULY
2011
0.0
10.0
20.0
30.0
40.0
50.0
[%]

Fig.3

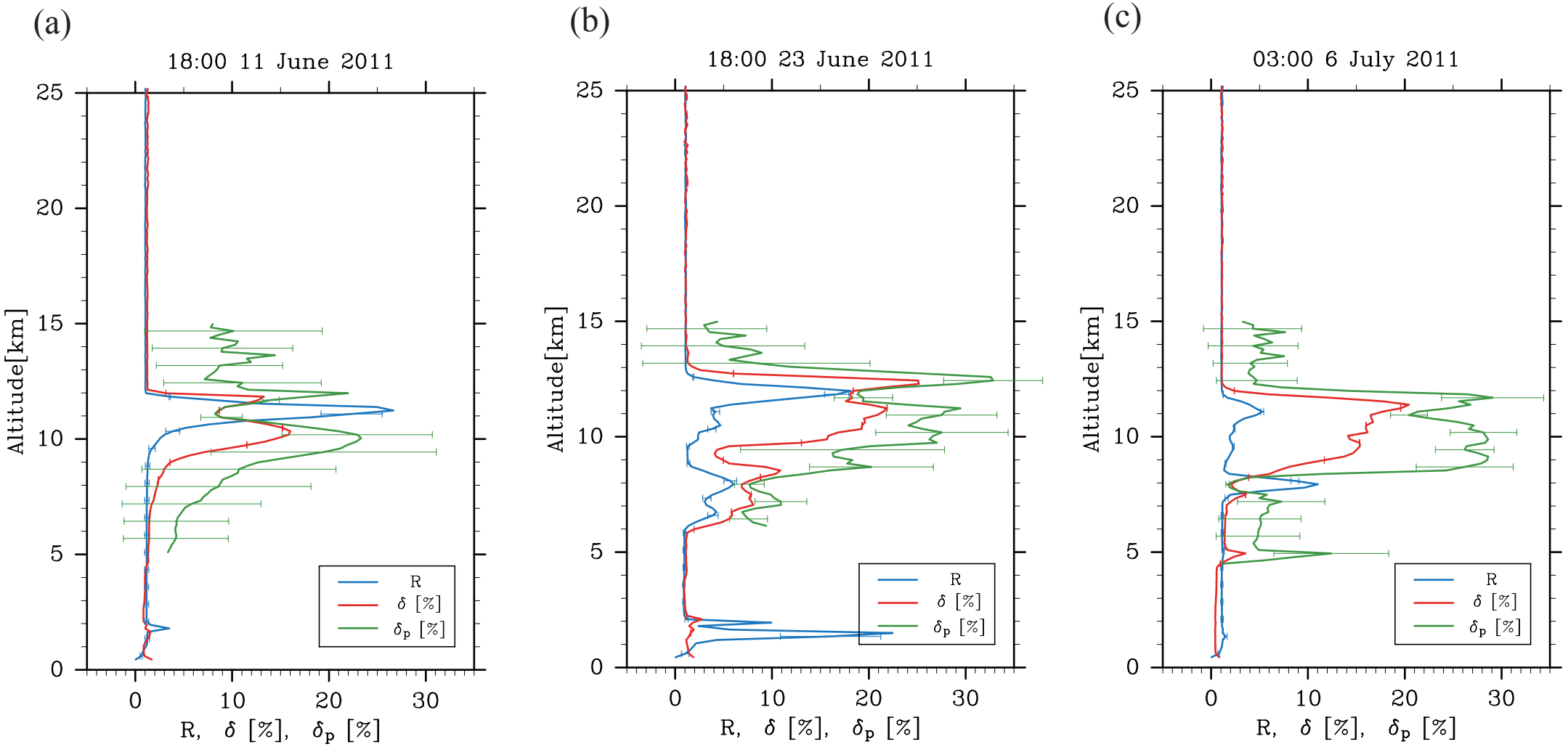
(a)
18:00 11 June 2011
(b)
18:00 23 June 2011
(c)
03:00 6 July 2011
Altitude[km]
R, δ [%], δp [%]
R
δ [%]
δp [%]
0
5
10
15
20
25
0
10
20
30

Fig. 4

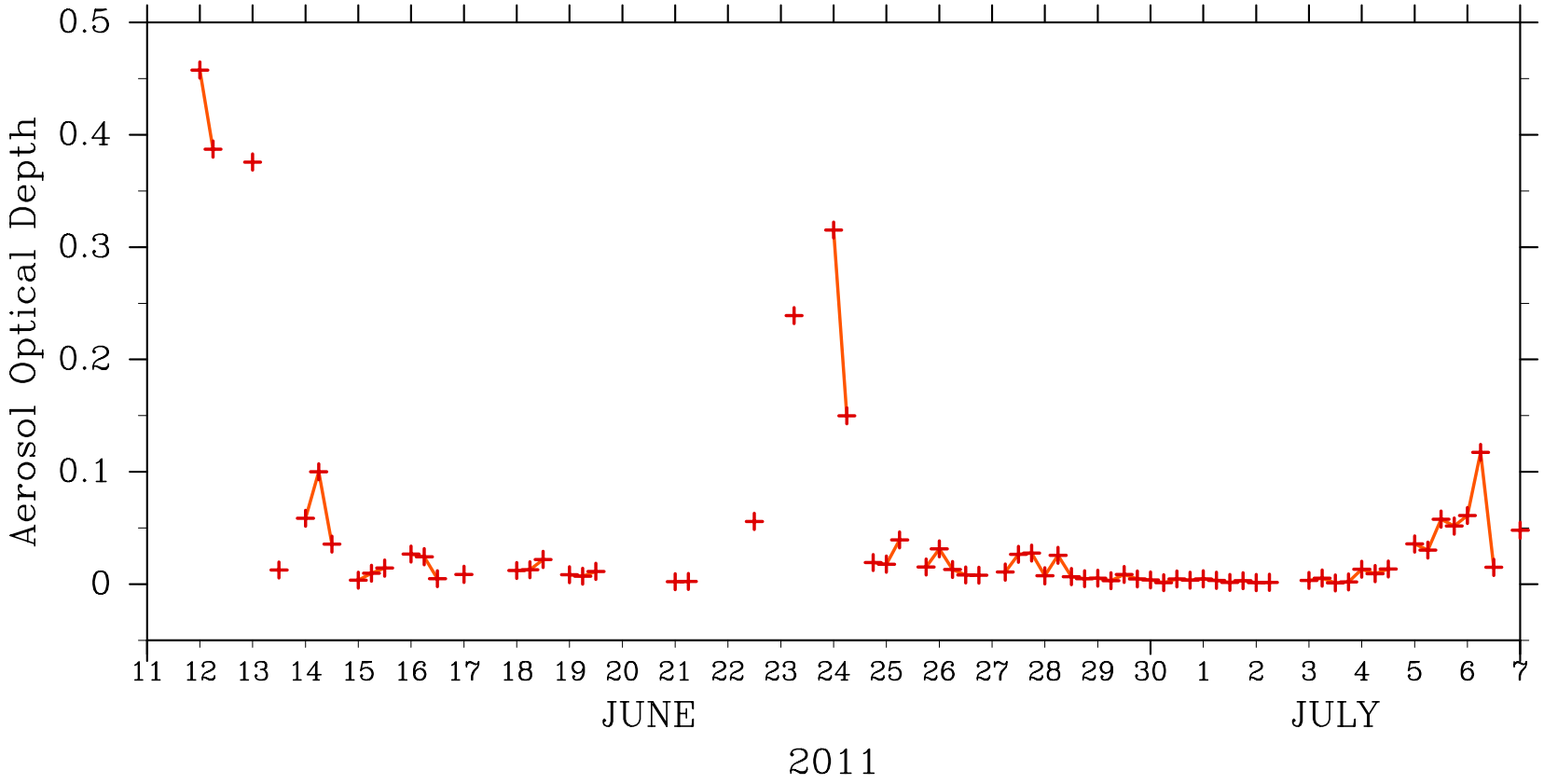
Aerosol Optical Depth
0.5
0.4
0.3
0.2
0.1
0
11 12 13 14 15 16 17 18 19 20 21 22 23 24 25 26 27 28 29 30 1 2 3 4 5 6 7
JUNE
JULY
2011

Fig.5

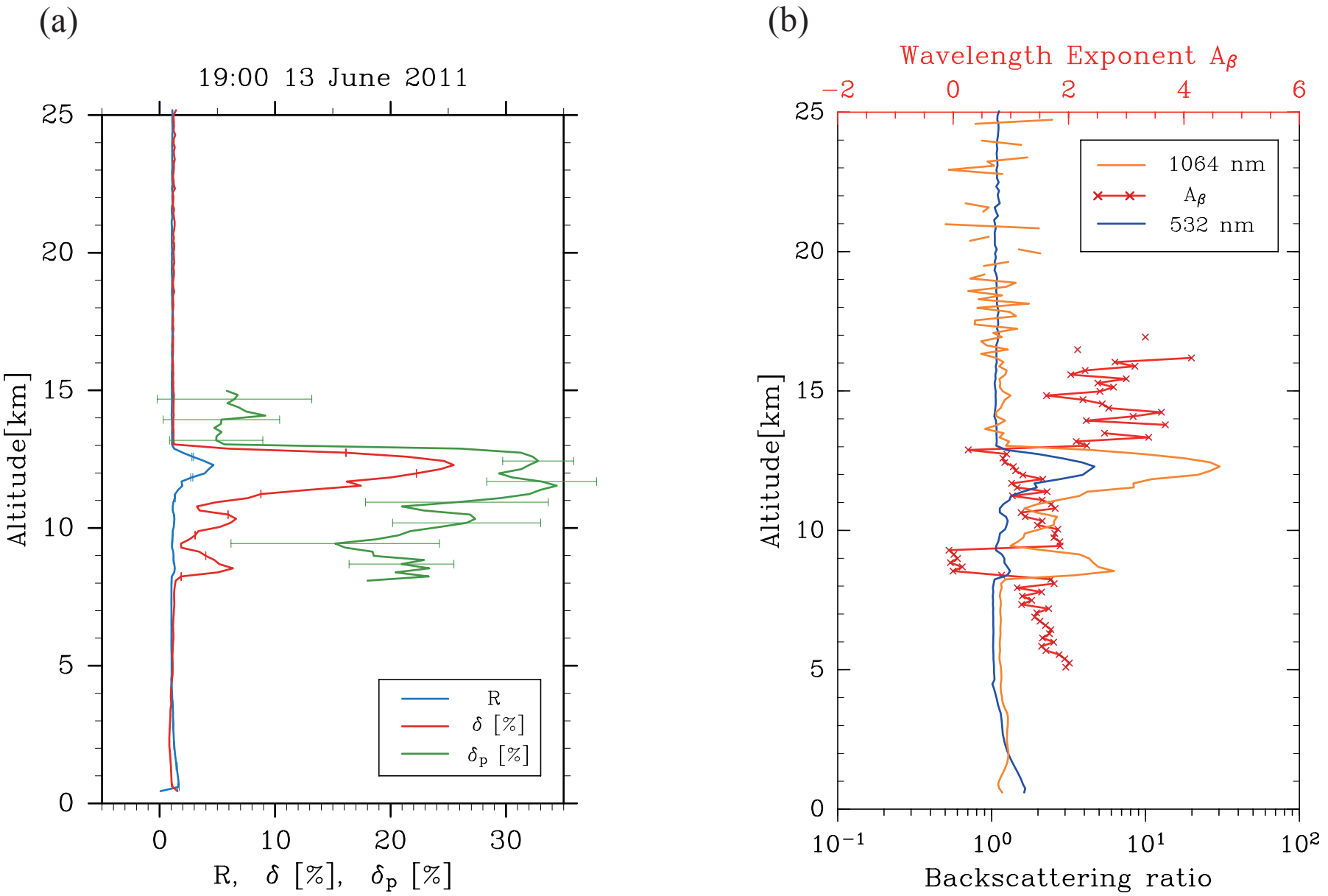
(a)
19:00 13 June 2011
Altitude[km]
R, δ [%], δp [%]
R
δ [%]
δp [%]
(b)
Wavelength Exponent Aβ
1064 nm
Aβ
532 nm
Backscattering ratio

Fig. 6